Ancient TL

A periodical devoted to Luminescence and ESR dating

June 2023, Volume 41 No.1

Ancient TL

Started by the late David Zimmerman in 1977

Ancient TL

Reducing computation time in the R-package 'BayLum'

Frederik Baumgarten[1]*, Anne Philippe[2], Guillaume Guérin[3], Sebastian Kreutzer[4,5]

[1] Department of Physics, Technical University of Denmark, DTU Risø Campus, Denmark

[2] Laboratoire de Mathématiques Jean Leray, Université de Nantes, 2 rue de la Houssinière,
BP 92208 44322 Nantes Cedex 3, France

[3] Université de Rennes, CNRS, Géosciences Rennes, UMR 6118, 35000 Rennes, France

[4] Institute of Geography, Ruprecht-Karl University of Heidelberg, 69120 Heidelberg, Germany

[5] Archéosciences Bordeaux, UMR 6034, CNRS-Université Bordeaux Montaigne, Pessac, France

*Corresponding Author: fhaba@dtu.dk

Abstract

'BayLum' is an R-package that facilitates the application of Bayesian models to the field of OSL dating. Here we present two recent feature updates to 'BayLum', significantly reducing computation time and improving general use. The first feature allows users to parallelize the computations involved in the MCMC sampling of values, while the second introduces the ability to extend a 'BayLum' model, which has run to completion without converging. All updates are automatically available with 'BayLum' v0.3.1.

Keywords: Age model, Chronology, MCMC algorithm, Luminescence dating, OSL

1. Introduction

'BayLum' is an R – package (R Core Team, 2022) that gives users the tools to easily apply the Bayesian models presented in Combès et al. (2015) and Combès & Philippe (2017) to luminescence dating data. See, for example, the work of Heydari et al. (2020), where an OSL chronology is provided for the paleolithic site of Mirak, Iran, using 'Bay-Lum'. In this work, they showed that the age uncertainty can be reduced significantly by imposing stratigraphic order – a feature of 'BayLum'. Since the introduction of 'BayLum' (Philippe et al., 2019), 'BayLum' has grown by drawing resources from the ever-developing R-landscape around it. The

latest iteration of 'BayLum' (v0.3.1) (Christophe et al., 2023) now employs `'runjags'` (Denwood, 2016) as the R to JAGS (Plummer, 2003) facilitator, which has made possible two key features of 'runjags' to be used inside 'BayLum': (i) MCMC-sampling parallelization and (ii) the ability to extend a model (drawing additional MCMC samples after a model has already run to completion). This paper will highlight these two new features of 'BayLum' and show examples of how to use them.

2. Problem: Stationary distributions require long run times

The Bayesian models produced with 'BayLum' infer parameter estimates (such as equivalent dose and age) from marginal posterior distributions of these parameters. This is to say that 'BayLum' takes the output of the Bayesian approach, a posterior distribution, and evaluates the dimensions of individual variables. 'BayLum' constructs these distributions via Markov Chain Monte Carlo sampling. The result of the MCMC sampling is a chain of values, each link consisting of a combination of values from all parameters in the Bayesian model. A distribution can then be constructed for each parameter, given its value in each link. To let the MCMC converge on the solution, we skip a number of the first iterations (burn-in phase) and only then begin constructing the distributions. To be confident in the results, the distributions must be stationary – that is, the location and shape of each distribution must not change if we draw additional samples. 'BayLum' assesses if distributions are stationary and independent of initialization of the MCMC by construct-

ing multiple chains instead of one. If the distributions from each chain agree with each other, we can be confident that the chains have converged to a single solution. By default, 'BayLum' uses three MCMC chains – a suitable balance between the power to detect non-convergence and the computational resources required (the number of chains is fully customizable by the user). 'BayLum' formalizes the question of convergence by incorporating as output the Rubin and Gelman diagnostic (Gelman & Rubin, 1992), which compares within-chain and between-chain variance. A common rule of thumb is that the upper 95 % credible interval limit of this diagnostic value indicates convergence when below 1.05.

For many practical applications of OSL dating, the number of iterations (or links in each chain) required to reach convergence is high (>500 000) – and higher still when 'BayLum' models incorporate many OSL samples as is the case with high-resolution chronologies. Because MCMC chains are to be processed consecutively, the overall process can become very time-consuming. For example, using a computer equipped with a 11th Gen i7-1185G7 clocking at 3.0 GHz (which has a relatively high single-core threading performance rating), runtimes can extend beyond several days. Furthermore, even when a model completes, not all of the model's parameters may have converged – a result which could require a complete re-run of the 'BayLum' modelling function.

3. 'BayLum' feature: MCMC parallelization

Previous versions of 'BayLum' could only process MCMC chains consecutively using a single processor core. With parallelization, it is now possible to assign n chains out onto n CPU processor cores. This allows each chain to be processed concurrently, and the runtime will (ideally) approach 1/n when compared to the time for running n chains using a single core. We tested this using 'BayLum' models where OSL example sets GDB3 and GDB5 were used (both included with the 'BayLum' package) to produce 2-sample models. Figure 1A shows that when running 4 000 total iterations per chain, we see a significant runtime reduction when running the model using parallelization (`jags_method = "rjparallel"`) as compared to using only a single CPU core (`jags_method = "rjags"`). Reduction increases with the number of MCMC chains constructed in the model, which is what we expect. We observed a reduction of 65 % for a 3-chain setup and 72 % for a 4-chain setup. The minor differences we see from the theoretical 1/n-rule most likely arise from runtime inside the 'BayLum' model functions, which is not due to the iteration of MCMC sampling. We also see from Figure 1B that this reduction is consistent with increasing numbers of iterations. Example 1 (Sec. 3.1) shows how to apply parallelization in 'BayLum' v0.3.1. Note that our model testing was carried out using the High-Performance Computing Cluster "Sophia" (Technical University of Denmark, 2019). The same code run on a desktop PC will show the same relative reductions but may show poorer runtimes, not only because of lower overall compu-

tation power but also - and more likely - due to advanced power throttling measures of modern CPU architectures implemented to prevent overheating in prolonged high-load situations.

3.1. Example 1

In the example below, which we kept as simple and user-friendly as possible, we show how to achieve parallelization. The key argument to set is `jags_method = "rjparallel"`. We use the example data included within 'BayLum' at installation.

Example 1: R Code: Achieving parallelization

```r
# MCMC parallelization example ####
# load libraries
library(BayLum)

# load example DataFiles GDB3 and GDB5
data(DATA1)
data(DATA2)

# combine DataFiles
# (we now have a 2-sample DataFile)
DF <- combine_DataFiles(DATA1, DATA2)

# construct BayLum model
BayLum_model <- AgeS_Computation(
  DATA = DF,
  SampleNames = c("GDB3", "GDB5"),
  Nb_sample = 2,
  BinPerSample = c(1, 1),
  LIN_fit = FALSE,
  Origin_fit = TRUE,
  Iter = 1e+03,
  burnin = 5e+02,
  adapt = 5e+02,
  n.chains = 3,
  jags_method = "rjparallel"
)
```

4. 'BayLum' feature: extend the 'BayLum' model

Unfortunately, 'BayLum' model chains will not always converge within the specified number of iterations. In previous versions of 'BayLum', the 'BayLum'-model would likely need to run again with a higher number of iterations. The added runtime of re-running 'BayLum' can now be avoided by extending the non-converged model instead of building it again from scratch. In this case, all non-converged model iterations are treated as burn-in. See Example 2 (Sec. 4.1) for an illustration of how to extend 'BayLum' models.
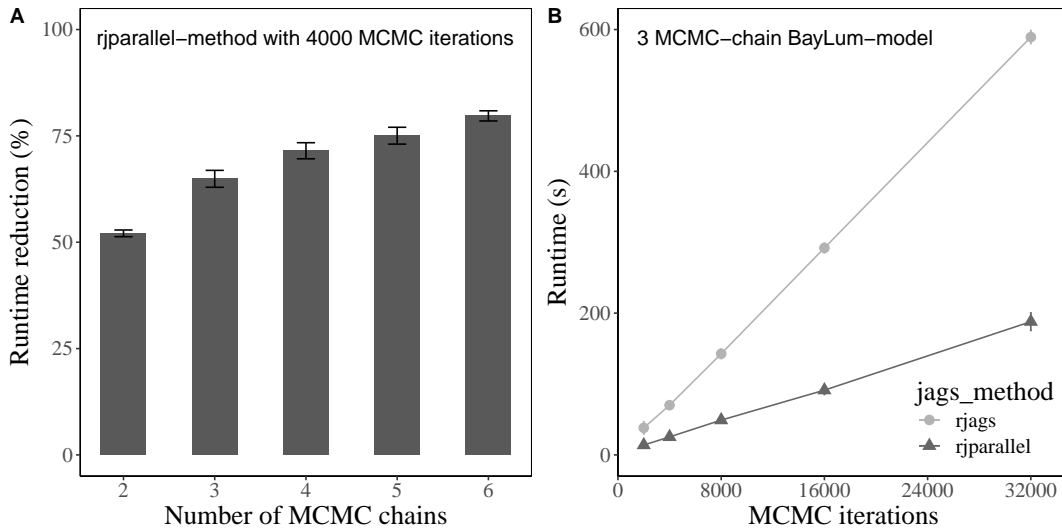
Figure 1: (A): Runtime reduction in percentage when running a 'BayLum' model with fixed iterations vs a varying number of MCMC chains using GDB3 and GDB5 example sets included within 'BayLum'. (B): Runtime in seconds vs the number of MCMC iterations for a 3-chain 'BayLum' model also using GDB3 and GDB5. All estimates show mean $\pm$ sd (n=8). To run the model, we used the High-Performance Computing cluster named "Sophia" owned by DTU. Arguments `"rjags"` and `"rjparallel"` entail whether 'BayLum' is run using a single CPU core ('rjags') or run in parallel on several cores ('rjparallel').

4.1. Example 2

In Example 1 (Sec. 3.1), a model was built to show how parallelization could be achieved. The Rubin and Gelman convergence diagnostics from that model reveal evidence that not all MCMC chains converged (see `"D (Dose)"` for GDB5, Table 1).

Table 1: Rubin and Gelman convergence diagnostics for three parameters of the 'BayLum'-model in Example 1. We show only the upper 95 % credible interval limit.

Sample	A (Age)	D (Dose)	sD (Stand. deviation)
GDB3	1.006	1.022	1.004
GDB5	1.007	1.065	1.000

However, we can now add iterations to the 'BayLum'-model in order to achieve convergence:

Example 2: R Code: Extending model

```
# extend MCMC sampling of BayLum-model
BayLum_model_extended <- AgeS_Computation(
  DATA = BayLum_model,
  SampleNames = c("GDB3", "GDB5"),
  Nb_sample = 2,
  BinPerSample = c(1, 1),
  LIN_fit = FALSE,
  Origin_fit = TRUE,
  Iter = 1e+04,
  burnin = 0,
  adapt = 5e02,
  jags_method = "rjparallel"
)
```

Rubin and Gelman's convergence diagnostics now show we can be confident about all the parameters (Table 2).

Table 2: Rubin and Gelman convergence diagnostics for three parameters of the 'BayLum' model from example 1 (Sec. 3.1). We show only the upper 95 % credible interval limit.

Sample	A (Age)	D (Dose)	sD (Stand. deviation)
GDB3	1.002	1.007	1.000
GDB5	1.001	1.010	1.004

5. Conclusions

In this report, we introduced two feature updates to the R-package 'BayLum'. Together, they allow users to parallelize MCMC sampling and extend BayLum-models - both features significantly reduce the time needed to build a viable 'BayLum'-model.

References

Christophe, C., Philippe, A., Kreutzer, S., Guérin, G., and Baumgarten, F. *BayLum: Chronological Bayesian Models Integrating Optically Stimulated Luminescence and Radiocarbon Age Dating. https://cran.r-project.org/package=BayLum*, 2023. URL https://cran.r-project.org/package=BayLum. R package version 0.3.1.

Combès, B. and Philippe, A. *Bayesian analysis of individual and systematic multiplicative errors for estimating ages with stratigraphic constraints in optically stimulated luminescence dating.* Quaternary Geochronology, 39: 24–34, 2017. ISSN 1871-1014. doi: 10.1016/j.quageo.2017.02.003. URL https://www.sciencedirect.com/science/article/pii/S1871101416300838.

Combès, B., Philippe, A., Lanos, P., Mercier, N., Tribolo, C., Guérin, G., Guibert, P., and Lahaye, C. *A Bayesian central equivalent dose model for optically stimulated luminescence dating.* Quaternary Geochronology, 28: 62–70, 2015. doi: 10.1016/j.quageo.2015.04.001.

Denwood, M. J. *runjags: An R Package Providing Interface Utilities, Model Templates, Parallel Computing Methods and Additional Distributions for MCMC Models in JAGS.* Journal of Statistical Software, 71: 1–25, 2016. doi: 10.18637/jss.v071.i09.

Gelman, A. and Rubin, D. B. *Inference from Iterative Simulation Using Multiple Sequences.* Statistical Science, 7: 457–472, 1992. ISSN 08834237. URL http://www.jstor.org/stable/2246093.

Heydari, M., Guérin, G., Kreutzer, S., Jamet, G., Kharazian, M. A., Hashemi, M., Nasab, H. V., and Berillon, G. *Do Bayesian methods lead to more precise chronologies? 'BayLum' and a first OSL-based chronology for the Palaeolithic open-air site of Mirak (Iran).* Quaternary Geochronology, 59: 101082, 2020. ISSN 1871-1014. doi: 10.1016/j.quageo.2020.101082. URL https://www.sciencedirect.com/science/article/pii/S1871101420300315.

Philippe, A., Guérin, G., and Kreutzer, S. *BayLum - An R package for Bayesian analysis of OSL ages: An introduction.* Quaternary Geochronology, 49: 16–24, 2019. doi: 10.1016/j.quageo.2018.05.009.

Plummer, M. *JAGS: A program for analysis of Bayesian graphical models using Gibbs sampling.* Proceedings of the 3rd International Workshop on Distributed Statistical Computing, Vienna, pp. 1–10, 2003.

R Core Team. *R: A Language and Environment for Statistical Computing.* R Foundation for Statistical Computing, Vienna, Austria, 2022. URL https://www.R-project.org/.

Technical University of Denmark. *Sophia HPC Cluster.* Research Computing at DTU, 2019. doi: 10.57940/fafc-6m81.

Reviewer

Geoff Duller

Ancient TL

Fine grain settling protocols for luminescence dating of museum objects sampled using the minimum extraction technique

Amber G. E. Hood[1*]

[1] Department of Geology, Lund University, Sweden

*Corresponding Author: amber.hood@geol.lu.se

Abstract

This paper communicates a suitable laboratory protocol for settling the 4 – 11 μm fine grain fraction for OSL dating of archaeological samples from museum artefacts sampled using the minimum extraction technique. It provides a step-by-step methodology to facilitate adapting this protocol for use more broadly and demonstrates its ability to successfully isolate the fine grain fraction from tiny samples.

Keywords: fine grain settling, Stokes' Law, minimum extraction technique, ceramics, museum artefacts, optically stimulated luminescence

1. Introduction

The use of polymineral fine grains in luminescence dating has long been established and routinely used where a larger grain size fraction cannot be obtained. With fine grain dating, using typically 4 – 11 μm grains, the alpha component of the dose rate, with a range of 20 μm, irradiates the entire grain, so there is no need to remove an alpha attenuation layer (Wintle 1997; p. 770). Of course, including the alpha component to the dose rate requires estimation of the alpha efficiency, which will vary depending on the composition of the sample.

The fine grain method was first described by Zimmerman (Zimmerman, 1967, 1971), although subsequent alterations have been made to the Zimmerman method (e.g. Frechen et al. 1996; Fleming 1975; Fleming 1979, p. 58-59). While the method has both its pros and cons (a full discussion of this topic is beyond the scope of this paper), it is still very useful in a wide range of applications in luminescence dating

today, particularly in archaeological settings (e.g. Anderson & Feathers 2019; Feathers 2009; Janz et al. 2015; Zink & Porto 2005).

The minimum extraction technique (MET) and extended MET sampling protocols are used to optimize OSL dating of archaeological artefacts housed in museum collections by extracting minute sample sizes (Hood & Schwenninger 2015; Hood 2022). MET protocols generally yield a sufficient quantity of fine grains for dating; however, as is to be expected, the process for isolating the 4 – 11 μm grain size fraction from the MET sample necessitates an adapted protocol compared to more standardised fine grain protocols, owing to the tiny sample sizes being worked with. Below, this adapted methodology, using the principle of Stokes' Law, is presented.[1]

2. Methodology: Fine grain sample preparation

Samples extracted using the (extended) MET protocol are in the form of drilled ceramic powder. A four-step process, as set out below, allows accurate isolation of the 4 – 11 μm fine grain fraction from the bulk MET sample.

Step 1: Dry sieving. When the MET sample is initially sieved (using small mesh or electro-formed hand held sieves[2]) to extract the coarse grain fraction, the < 90 μm grain size fraction is retained for the fine grain technique.[3]

---

[1]It is also possible to sieve out the polymineral fine grain fraction of a MET sample using size specific electro-formed sieves, however the cost of such equipment and the labour-intensive cleaning process can be a deterrence.

[2]An electro-formed sieve is created by electro-deposition of a metal that allows precision construction of very fine sieves.

[3]It should be noted that other fine grain methodologies frequently incorporate an H_2O_2 and/or HCl wash into their fine grain preparation. However this has, to date, been avoided for MET samples owing to the extremely

Step 2: First settling. To isolate the $4-11$ µm fraction from the < 90 µm fraction, it is necessary to settle the grains in a water column, using Stokes' law to determine the correct settling times for procuring this size fraction. The first settling step requires the removal of the ~ 12-90 µm grain size fraction using Stokes' Law (see, for example, Batchelor 2010, p.230-235). A calculation was made to determine the time it would take grains > 11 µm to settle in a solution of deionised water, based on the density and viscosity of the water, the temperature of the water, and the height of the graduated cylinder in which they were being settled.[4]

After adding the water to the cylinder, the MET sample is placed on a sheet of weighing paper, then rolled into a funnel so as to rapidly shoot the sample directly into the centre of the water column to avoid it adhering to the cylinder walls. A rapid movement of the sample into the water column is necessary to help break the surface tension of the water which can hold the MET sample owing to its extremely low mass. In the event of the sample staying on the surface of the water column, the surface tension can be broken by gently agitating it with a pin (or similar).

A 10 mL glass graduated cylinder is used for this first settling step owing to both its small size being the most appropriate for ease of dealing with MET-sized samples, and the glass facilitating the decanting of the sample.[5] Resulting settling times are presented in Table 1; the settling times presented in Table 1 and Table 2 are based on an average temperature of $19\,°C$; however, the ambient temperature of the deionised water was observed to fluctuate between $19\,°C$ and $26\,°C$ and thus the water used for each sample was measured prior to settling, and the exact temperature was used to calculate settling times).

Cylinder volume	Cylinder height	Drop height (average)	Settling time
10 mL	8.6 cm	4.3 cm	6 min 46 sec

Table 1: Settling times (at $19\,°C$) to remove the $11-90$ µm grain size fraction.

At the end of the allotted settling time, the water column now holds in suspension grains ≤ 11 µm, and the base of the cylinder holds the > 11 µm grains. The water

must now carefully be decanted into an identically sized graduated cylinder, leaving the settled material (i.e. the > 11 µm material remaining at the bottom on the cylinder) in approximately 1 mm of water, ensuring that none of the settled material is transferred during the decanting process. Upon being decanted into the next cylinder, the second step should begin immediately.[6]

Step 3: Second settling. Once the water in which the ≤ 11 µm fraction is suspended is decanted into a glass 10 ml cylinder, the next step to isolate the $4-11$ µm grains from the ≤ 3 µm fraction begins immediately. As we are now isolating the $4-11$ µm grain size fraction, the settling times are adjusted accordingly (see Table 2). Once the settling time is complete, the water column (which now contains grains 3 µm or smaller in suspension) can be poured off and discarded, or kept according to preference. The material now in the base of the cylinder is the desired $4-11$ µm grain size fraction, and can now be collected in Step 4.

Cylinder volume	Cylinder height	Drop height (average)	Settling time
10 mL	8.6 cm	4.3 cm	51 min 8 sec

Table 2: Settling times (at $19\,°C$) to remove the $4-11$ µm grain size fraction.

Step 4: Preparation of liquid suspension. The material left in the base of the cylinder after Step 3, that is, the $4-11$ µm grain size fraction, is now carefully washed into a small glass vial using acetone[7] and is then stoppered and kept in liquid suspension until fine grain aliquot preparation is carried out.

Upon the completion of the four steps above the sample is then ready to be mounted as fine grain aliquots. To make an aliquot, as with the coarse grain technique, a small aluminium disc 10 mm in diameter and 0.5 mm thick is used. The disc is placed in a small glass vial (measuring 12 mm in diameter and c. 38 mm in height, to facilitate subsequent removal of the aliquot). However, it is essential that the disc is lying flat on the base of the vial so that the fine grains cannot become trapped under the disc, which could affect the preheating of the aliquots when being measured. This can be achieved by placing ~ 0.25 mL of acetone in the vial first and then placing the aluminium disc on top of the acetone, as this creates a suction force, ensuring the disc remains at the bottom of the vial. The glass vial containing the sample

---

small sample mass and the likelihood of sample loss if another treatment step is introduced at this stage. However, ultimately, this decision should be made based on the individual nature of the material one is working with, i.e. a large carbonate and/or organic component to the sample may necessitate employing these additional steps, even at the expense of precious sample loss.

[4] A selection of online calculators are available to facilitate the calculation of settling times.

[5] If the sample is irreplaceable, i.e. there is no ability to obtain more, it may be preferable to use new glass cylinders only in MET fine grain preparation, in order to avoid potential sample contamination which could occur during cleaning between samples since fine grain material is invisible to the naked eye and MET samples are usual a 'once-off' without the possibility of obtaining more material in the event of sample contamination. However, the environmental and financial impact must also be considered for such a decision, and it is perhaps better practice to only use a new cylinder on particularly valuable/irreplacable sample.

[6] The ~ $12-90$ µm fraction can be washed into a glass vial and stored in liquid suspension if required.

[7] It is also possible, of course, to use acetone instead of distilled water in the aforementioned steps, and indeed there is an argument to be made for this facilitating drying and settling. However, owing to additional considerations (costs and additional chemical use), our preference has been to only use acetone in this final step. The minute amount of mixing between water and acetone in this step has, in our observation, not hindered aliquot preparation. Additionally, if acetone is being used instead of water in all steps, then the potential issue with surface tension noted above for distilled water is usually avoided.
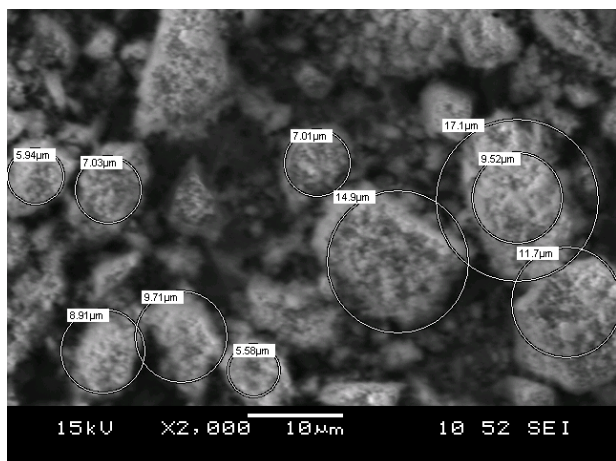
Figure 1: SEM image showing distribution of fine grain sizes for the brick test sample after settling to isolate the $4-11$ μm fraction.

suspended in acetone prepared in Step 4 above is then gently agitated to ensure that all grains are once again in suspension (the vial should not be inverted so as not to trap fine grains around the lid) and, using a disposable pipette, 1 mL of liquid sample is added to the vial and is left to settle onto the disc.[8] This vial is then left open and placed in a fume cupboard so that the acetone can dry off. Once the acetone is evaporated, the disc can be removed carefully from the vial using tweezers. The aliquot will now have a thin monolayer of fine grains which have settled upon its surface during the evaporation process and is ready for measurement.[9]

3. Results

The fine grain preparation process was tested to ensure that it was accurately isolating the 4–11 μm grain size fraction. For a test sample, once aliquots were prepared a selection were examined under a scanning electron microscope (SEM) to quantify grain sizes.

SEM examinations showed that the described methodology is suitable for isolation of fine grains for OSL dating. The majority of grains observed were within the $4-11$ μm grain size fraction, although with some slightly smaller (~ 3 μm) and some slightly larger ($\sim 12-17$ μm) grains occurring too (Figure 1). Given that this slightly increased

grain size distribution is inevitable due to the use of average drop heights and assumption of spherical grain geometry upon which Stokes' law is based, this variance is considered acceptable, and even the slightly larger grains are still smaller than the alpha range, i.e. 20 μm.

4. Conclusion

This paper has presented a step-by-step methodology to isolate fine grains for OSL measurement from samples obtained using the MET or extended MET protocol. It provides a means by which to maximise the quantity of measurable material from OSL dating when working with museum objects — for which only minute sample sizes can be obtained — by making use of the multi-mineral fine grain fraction as well as coarse grain mineral fractions. The methodology can be readily and easily implemented by other luminescence practitioners working with minute museum samples, or indeed wherever only small sample sizes are available for luminescence dating.

Acknowledgments

---

[8]In standard fine grain aliquot preparation, it is necessary at this step to be very careful not to use too much liquid and thus allow too many fine grains to adhere to the disc. It is often also necessary, in standard methodology, to dilute the sample suspension. However, due to the very small amounts sampled during MET extraction, it has been observed that the quantity of fine grain material usually retained from a MET sample, when prepared in accordance with the steps outlined above, produces a good grain density for aliquot making (i.e. not too cloudy, that is, not too many grains present), which means it is not necessary to dilute the sample. However, as there can be a considerable amount of variation between different sample types, practitioners may still find dilution necessary for some samples.

[9]This monolayer should not be visible to the naked eye, and thus it is not necessary to attempt to add more grains via additional liquid suspension.

References

Anderson, S. L. and Feathers, J. K. *Applying luminescence dating of ceramics to the problem of dating Arctic Archaeological sites.* Journal of Archaeological Science, 112: 10503, 2019.

Batchelor, G. K. *An Introduction to Fluid Dynamics.* Cambridge University Press, Cambridge, 2010.

Feathers, J. K. *Problems of ceramic chronology in the Southeast: does shell-tempered pottery appear earlier than we think?* American Antiquity, 74: 113–142, 2009.

Fleming, S. J. *Supralinearity Corrections in Fine-grain Thermoluminescence Dating: A Re-appraisal.* Archaeometry, 17: 122–129, 1975.

Fleming, S. J. *Thermoluminescence Techniques in Archaeology.* Clarendon Press, Oxford, 1979.

Frechen, M., Schweitzer, U., and Zander, A. *Improvements in Sample Preparation for the Fine Grain Technique.* Ancient TL, 14 (2): 15–17, 1996.

Hood, A. G. E. *The extended minimum extraction technique: an update on sampling protocols.* Ancient TL, 40(2): 8–10, 2022.

Hood, A. and Schwenninger, J.-L. *The Minimum Extraction Technique: A New Sampling Methodology for Optically Stimulated Luminescence Dating of Museum Ceramics.* Quaternary Geochronology, 30: 381–385, 2015.

Janz, L., Feathers, J. K., and Burr, G. S. *Dating surface assemblages using pottery and eggshell: assessing radiocarbon and luminescence techniques in Northeast Asia.* Journal of Archaeological Science, 57: 119–129, 2015.

Wintle, A. G. *Luminescence dating: laboratory procedures and protocols.* Radiation measurements, 27(5-6): 769–817, 1997.

Zimmerman, D. W. *Thermoluminescence from Fine Grains from Ancient Pottery.* Archaeometry, 10(1): 26–28, 1967.

Zimmerman, D. W. *Thermoluminescent Dating Using Fine Grains from Pottery.* Archaeometry, 13(1): 29–52, 1971.

Zink, A. and Porto, E. *Luminescence Dating of the Tanagra Terracottas of the Louvre Collections.* Geochronometria, 24(2): 21–26, 2005.

Reviewer

Jim Feathers

Thesis Abstracts

Chloé Bouscary

Sub-Quaternary Himalayan tectonics inferred from luminescence thermochronometry

December 2022

Institute of Earth Surface Dynamics, University of Lausanne, Lausanne, Switzerland

Degree: Ph.D.

Supervisor: Georgina King

Luminescence thermochronometry is a very low-temperature thermochronometer that allows reconstruction of the thermal histories of the upper first few km of the Earth's crust within the last few 100 kyr (late Quaternary); a spatial and temporal scale hitherto at the sensitivity limit of other methods. Despite the potential of this method for deriving changes in landscape and subsurface evolution, it has until now never been applied to a large-scale study area, or been validated as a multi-thermochronometer approach.

I calibrated the multi-luminescence measurement protocol for feldspar thermochronometry by analysing three sets of samples (independently known thermal histories samples, synthetic thermal history samples created following irradiation at high temperature in the laboratory, and unknown-thermal history samples). As the reconstruction of a sample's thermal history depends on the thermal kinetic parameters extracted from isothermal decay experiments, I tested the validity of thermal kinetic parameters obtained from different combinations of isothermal holding data by trying to recover the sample's temperature. I found that the temperatures inferred from inverting the data vary depending on the combination of isothermal holding temperatures used for thermal kinetic parameter derivation, and that the inclusion of isothermal holding data above 250 °C result in kinetic parameters that underestimate modelled temperatures. For appropriate thermal kinetic parameter derivation, and thus accurate thermochronometric data, I recommended using a new protocol with four isothermal holding temperatures between 190 and 250 °C.

The improved multi-luminescence thermochronometry method was then used as a tool to constrain the late Quaternary exhumation history of the Himalayas, where two end-member competing models have been proposed to describe the kinematics of the central Nepal Himalayas in the last few Myr. They differ in their interpretations of which surface breaking faults accommodate current shortening and the kinematics responsible for driving rapid exhumation in the topographic transition zone around the Main Central Thrust (MCT). These locally higher uplift and erosion rates in the High Himalaya could reflect thrusting over a midcrustal ramp with the growth of a Lesser Himalaya duplex at midcrustal depth, or out-of-sequence thrusting along the front of the High Himalaya, possibly driven by climatically controlled localized exhumation. To address this debate, I successfully measured and analysed more than 100 rock samples with luminescence thermochronometry (10^{4-5} yr), filling the temporal gap between GPS measurement, palaeoseimic ($\leq 10^2$ yr), Holocene fluvial terrace records (10^{3-4} yr) and geological estimates ($\geq 10^6$ yr) of exhumation rates.

I first focussed on the Sub-Himalayas, the most frontal fold-and-thrust belt of the Himalayan orogen. Samples collected along six transects across the Siwalik foothills yield exhumation rates of $\sim 3-11$ mm/yr over the past ~ 200 kyr, which convert to thrust slip rates of $\sim 6-22$ mm/yr. Comparing these rates with geodetic convergence rates indicates that at least half of the Himalayan convergence is accommodated by the Sub-Himalayan fold-and-thrust belt, and particularly by the Main Frontal Thrust, since the late Quaternary, consistent with this fault being a high seismic hazard zone. Data also record exhumation rates on local Sub-Himalayan intra-wedge thrusts throughout the same time period, implying that internal deformation of the orogenic wedge and strain partitioning may have occurred, potentially endangering an entire population.

I then compared existing low and medium-temperature thermochronometric data (^{40}Ar/^{39}Ar on muscovite, apatite and zircon (U-Th)/He, and apatite and zircon fission track), to newly acquired luminescence thermochronometry data from the High Himalaya of central Nepal. All of the thermochronometric data show younger ages and higher exhumation rates around the topographic transition and the MCT zone. For the higher temperature thermochronometers, a continuous trend towards younger ages from the Lesser Himalaya through the topographic transition and the MCT zone suggest that the duplexing model best describes the thermochronometric ages of this study area on Myr timescales. However, the luminescence thermochronometry data highlight a systematic sharp transition at the MCT, pointing to out-of-sequence activity at this tectonic boundary on 100-kyr timescales. Whether this difference in tectonic model between the two timescales is due to low resolution of the higher temperature thermochronometers, shallow isotherms deflected by fluid circulation and hot spring activity near the

MCT, or to a change in tectonic regime during the last 200 kyr, out-of-sequence activity of the MCT needs to be considered in seismic hazard models as it could put the local population at risk.

A PDF of this thesis can be obtained by contacting the author: chloe.bouscary@unil.ch

---

Christopher Garcia
Development of an Instrument for Spatially Resolved, Optically Stimulated Luminescence Dosimetry of Cobble and Dosimeter Surfaces
June 2023
Department of Physics, East Carolina University, Greenville, NC, USA

Degree: Ph.D.
Supervisor: Regina DeWitt

Optically stimulated luminescence (OSL) dosimetry is a method used to determine the amount of energy stored within a crystalline insulator due to ionizing radiation. At its most fundamental, OSL dosimetry requires optical stimulation to induce a sample to emit luminescence, a light detection apparatus to collect the luminescence signal, and a calibrating radiation source to convert the acquired signal into an equivalent dose. Conventional instruments have successfully integrated these components to perform OSL dosimetry on sediment and dosimeters. In this dissertation, an instrument was developed that allows dose-mapping: LuCIDD (Luminescence instrument with Confocal and Imaging unit for Dating and Dosimetry) is based on the principles of a confocal microscope. This dissertation outlines the requirements for spatially resolved dosimetry mapping and describes the design and construction of LuCIDD. Tests of the integrated lasers' ability to perform spatially resolved stimulating measurements were made by measuring their focal spot size, power density, and penetration depth. Used for calibration, the built-in X-ray source's energy spectrum, uniformity, and dose rate were characterized. The minimum resolution and stimulation time for measurements were determined, quantifying the amount of time to complete a dose map of a sample's surface. Lastly, LuCIDD's ability to recover a known applied dose from single points was verified to provide a proof-of-concept for future dose-mapping measurements.

Bibliography

Compiled by Sebastien Huot

From December 1, 2022 to May 31, 2023

<u>**Various geological applications**</u>

- aeolian

Dabhi, M., Thakkar, A., Chavan, A., Chauhan, G., Bhagora, R., Chauhan, N., Shukla, A.D., Bhandari, S., Thakkar, M.G., 2022. Mid-late Holocene climatic reconstruction from coastal dunes of the western Kachchh, India. Quaternary International 642, 29-40, http://doi.org/10.1016/j.quaint.2021.09.011

Feng, M., Lü, T., Sun, J., Cui, C., 2023. Optically stimulated luminescence dating and paleoclimatic implications of the Holocene dune sands in the Hunshandake Sandy Land, Northeast China. Palaeogeography, Palaeoclimatology, Palaeoecology 615, 111469, http://doi.org/10.1016/j.palaeo.2023.111469

Gao, Y., Zhang, K., Wu, Z., Tian, T., Li, B., 2023. Factors controlling the Early-Mid Holocene aeolian sediment accumulation in the Pum Qu catchment and environmental implications for the southern Tibetan Plateau. Quaternary International 652, 17-32, http://doi.org/10.1016/j.quaint.2023.01.013

Liu, B., Zhao, H., Jin, H., Liang, A., Sun, A., Zhang, X., Zhang, C., Jin, J., Yang, H., Li, S., 2023. Quantitative estimates of Holocene precipitation from aeolian sand-palaeosol sequences across the Ordos Plateau, northern China, based on surface soil geochemistry. CATENA 229, 107232, http://doi.org/10.1016/j.catena.2023.107232

Mescolotti, P.C., Giannini, P.C.F., Pupim, F.d.N., Sawakuchi, A.O., Ladeira, F.S.B., Assine, M.L., 2023. The largest Quaternary inland eolian system in Brazil: Eolian landforms and activation/stabilization phases of the Xique-Xique dune field. Geomorphology 420, 108516, http://doi.org/10.1016/j.geomorph.2022.108516

Ohata, K., Hori, K., Ishii, Y., Tamura, T., 2023. Sedimentary characteristics and formation of riverine source bordering dunes in a humid region: an example from the lower reaches of Kiso River, central Japan. Geomorphology 426, 108602, http://doi.org/10.1016/j.geomorph.2023.108602

Robins, L., Roskin, J., Marder, O., Edeltin, L., Yu, L., Greenbaum, N., 2023. Geomorphic, environmental, and archeological significance of Last Glacial Maximum to middle Holocene dune damming, northwestern Negev dunefield margin, Israel. Quaternary Science Reviews 308, 108098, http://doi.org/10.1016/j.quascirev.2023.108098

Sevink, J., Wallinga, J., Reimann, T., van Geel, B., Brinkkemper, O., Jansen, B., Romar, M., Bakels, C.C., 2023. A multi-staged drift sand geo-archive from the Netherlands: New evidence for the impact of prehistoric land use on the geomorphic stability, soils, and vegetation of aeolian sand landscapes. CATENA 224, 106969, http://doi.org/10.1016/j.catena.2023.106969

Shu, P., Kang, S., Shi, Z., Grimley, D.A., Zhang, Z., Zhao, J., Wang, H., Zhou, W., An, Z., 2023. Southward migration of the monsoonal rainbelt hinders paleosol development and preservation in north-central China dunefield after the Middle-Late Holocene Transition. Quaternary Science Reviews 301, 107919, http://doi.org/10.1016/j.quascirev.2022.107919

Zhang, J., E, C., Yang, F., XianBa, j., Shi, Y., Xie, L., 2023. OSL ages and pedogenic mode of Kobresia mattic epipedon on the northeastern Qinghai-Tibetan Plateau. CATENA 223, 106912, http://doi.org/10.1016/j.catena.2023.106912

- alluvial fan

Ginter, A., Piech, W., Krąpiec, M., Moska, P., Sikorski, J., Hrynowiecka, A., Stachowicz-Rybka, R., Cywa, K., Piotrowska, N., Mroczkowska, A., Tołoczko, W., Okupny, D., Mazurkevich, A., Kittel, P., 2023. Intense and quick land relief transformation in the Little Ice Age: The age of accumulative fan deposits in Serteyka River Valley (Western East European Plain). Quaternary International 644-645, 160-177, http://doi.org/10.1016/j.quaint.2022.02.015

Sanjurjo-Sánchez, J., Viveen, W., Vega-Centeno Sara-Lafosse, R., 2022. Testing the accuracy of OSL and pIR IRSL dating of young geoarchaeological sediments in coastal Peru. Quaternary Geochronology 73, 101382, http://doi.org/10.1016/j.quageo.2022.101382

- cave

del Val, M., Alonso, M.J., Duval, M., Arriolabengoa, M., Álvarez, I., Bodego, A., Cheng, H., Hermoso de Mendoza, A., Aranburu, A., Iriarte, E., 2022. Luminescence and ESR dating of the sedimentary infill from the multi-level cave system of Alkerdi-Zelaieta (Navarre, N Spain). Quaternary Geochronology 73, 101380, http://doi.org/10.1016/j.quageo.2022.101380

Mahan, S., Wood, J.R., Lovelace, D.M., Laden, J., McGuire, J.L., Meachen, J.A., 2023. Luminescence ages and new interpretations of the timing and deposition of Quaternary sediments at Natural Trap Cave, Wyoming. Quaternary International 647-648, 22-35, http://doi.org/10.1016/j.quaint.2022.01.005

Vieira de Sousa, D., Spinola, D., dos Santos, J.C., Hatsui Tatumi, S., Yee, M., Aline Pessoa Oliveira, R., Eltink, E., do Vale Lopes, D., Spötl, C., Cherkinsky, A., Figueirado Reis, H., de Oliviera Silva, J., Auler, A., William da Cruz, F., 2023. Relict soil features in cave sediments record periods of wet climate and dense vegetation over the last 100 kyr in a present-day semiarid region of northeast Brazil. CATENA 226, 107092, http://doi.org/10.1016/j.catena.2023.107092

- coastal

Butuzova, E.A., Kurbanov, R.N., Taratunina, N.A., Makeev, A.O., Rusakov, A.V., Lebedeva, M.P., Murray, A.S., Yanina, T.A., 2022. Shedding light on the timing of the largest Late Quaternary transgression of the Caspian Sea. Quaternary Geochronology 73, 101378, http://doi.org/10.1016/j.quageo.2022.101378

Hidayat, R., Murray-Wallace, C.V., Jacobs, Z., 2023. Late Pleistocene evolution of Robe Range, southern Australia – The timing and carbonate source dynamics of coastal dune development. Marine Geology 456, 106987, http://doi.org/10.1016/j.margeo.2022.106987

Lin, P., Song, Y., Zhan, W., Tian, R., Wang, Z., Xu, X., Luo, L., Abbas, M., Lai, Z., 2023. Late Pleistocene to Holocene sedimentary history in the Pearl River Delta revealed by OSL and radiocarbon dating. CATENA 224, 106972, http://doi.org/10.1016/j.catena.2023.106972

McKenzie, K.A., Kelsey, H.M., Kirby, E., Rittenour, T.M., Furlong, K.P., 2022. Differential coastal uplift quantified by luminescence dating of marine terraces, central Cascadia forearc, Oregon. Quaternary Science Reviews 298, 107853, http://doi.org/10.1016/j.quascirev.2022.107853

Qiu, J., Jin, J., Wang, X., Wei, C., Zuo, X., Wei, J., 2022. OSL chronological evidence reveals one of the earliest island-type Neolithic sites in the coastal area of South China. The Holocene 33, 27-37, http://doi.org/10.1177/09596836221126126

Rahimzadeh, N., Tsukamoto, S., Thiel, C., Frechen, M., 2023. Progress and pitfalls of the SAR protocol for the quartz violet stimulated luminescence (VSL) signal: A case study from Sardinia. Quaternary Geochronology 75, 101433, http://doi.org/10.1016/j.quageo.2023.101433

Yoon, H.H., Kim, J.C., Yoo, D.-G., Lee, G.-S., Hong, S.-H., 2022. Multi dating approach of long marine core sediments from the south-eastern continental shelf of Korea: Comparison of SAR OSL, TT-OSL and pIRIR dates. Quaternary Geochronology 73, 101338, http://doi.org/10.1016/j.quageo.2022.101338

- earthquake (and fault related)

Abbas, W., Zhang, J., Tsukamoto, S., Ali, S., Frechen, M., Reicherter, K., 2023. Pleistocene-Holocene deformation and seismic history of the Kalabagh Fault in Pakistan using OSL and post-IR IRSL dating. Quaternary International 651, 42-61, http://doi.org/10.1016/j.quaint.2022.01.007

Gutiérrez, F., Deirnik, H., Zarei, M., Medialdea, A., 2023. Geology, geomorphology and geochronology of the coseismic? Emad Deh rock avalanche associated with a growing anticline and a rising salt diapir, Zagros Mountains, Iran. Geomorphology 421, 108527, http://doi.org/10.1016/j.geomorph.2022.108527

Jahan, N., Rana, Y.P., Singh, R.J., 2023. Structural evidences of active tectonics along Himalayan Frontal Thrust of northwest Himalaya: A case study along Kumia river section, Nainital, India. Journal of Earth System Science 132, 57, http://doi.org/10.1007/s12040-023-02078-1

Ma, Z., Peng, T., Feng, Z., Li, X., Song, C., Wang, Q., Tian, W., Zhao, X., 2023. Tectonic and climate controls on river terrace formation on the northeastern Tibetan Plateau: Evidence from a terrace record of the Huangshui River. Quaternary International 656, 16-25, http://doi.org/10.1016/j.quaint.2022.11.004

Malik, J.N., Mohanty, A., Sahoo, S., Gadhavi, M.S., Dhali, M., Arora, S., Naik, S.P., 2023. Signatures of 16th and 19th centuries paleo-earthquakes along the Himalayan Frontal Thrust (HFT), NW Himalaya, India: Implications to seismic hazard assessment. Quaternary International 656, 37-47, http://doi.org/10.1016/j.quaint.2023.02.001

- fluvial

Achyuthan, H., 2022. Middle to late Holocene alluvial history of the northeast monsoon dominated coastal tropical rivers of south India. Quaternary International 642, 63-72, http://doi.org/10.1016/j.quaint.2021.09.012

Be'eri-Shlevin, Y., Matmon, A., Rotstein, R., Schimmelpfennig, I., Benedetti, L., Geller, Y., Porat, N., Greenbaum, N., 2023. Denudation of the Golan Heights basaltic terrain using in-situ 36Cl and OSL dating. Geomorphology 430, 108649, http://doi.org/10.1016/j.geomorph.2023.108649

Chauhan, N., Sundriyal, Y., Kaushik, S., Chahal, P., Panda, D.K., Banerjee, D., Narayanan, A., Shukla, A.D., 2023. Chronology and paleoclimatic implications of the upper Ganga catchment floods since Marine Isotopic Stage-2. Palaeogeography, Palaeoclimatology, Palaeoecology 620, 111566, http://doi.org/10.1016/j.palaeo.2023.111566

Dabhi, M., Chavan, A., Thakkar, A., Chauhan, G., Bhagora, R., Chauhan, N., Shukla, A.D., Bhandari, S., 2022. Climatic history from early Weichselian (MIS 5D-C) valley-fill deposits and associated factors for basin sedimentation, mainland Kachchh, western India. Quaternary International 642, 17-28, http://doi.org/10.1016/j.quaint.2021.10.019

Guo, Y., Ge, Y., Mao, P., Liu, T., 2023. Reconstruction of mid-Holocene extreme flood events in the upper Minjiang River valley, eastern Tibetan Plateau, China. Palaeogeography, Palaeoclimatology, Palaeoecology 617, 111517, http://doi.org/10.1016/j.palaeo.2023.111517

Hernando-Alonso, I., Moreno, D., Ortega, A.I., Benito-Calvo, A., Alonso, M.J., Parés, J.M., Martínez-Fernández, A., Carbonell, E., Bermúdez de Castro, J.M., 2022. ESR chronology of the fluvial sequence of Cueva del Silo (Sierra de Atapuerca, Spain). Quaternary Geochronology 73, 101374, http://doi.org/10.1016/j.quageo.2022.101374

Kumar, K., Sharma, A., Srivastava, P., Thakur, B., 2023. Implications for catchment weathering, provenance, and climatic records from a late Pleistocene to present sedimentary sequence in Gujarat, India. Quaternary Research 111, 148-165, http://doi.org/10.1017/qua.2022.39

Lombardi, R., Davis, M.A.L., 2022. Incorporating alluvial hydrogeomorphic complexities into paleoflood hydrology, magnitude estimation and flood frequency analysis, Tennessee River, Alabama. Journal of Hydrology 612, 128085, http://doi.org/10.1016/j.jhydrol.2022.128085

Pang, H., Gao, H., Eduardo, G., Li, F., Pan, B., 2023. Fluvial-aeolian interactions in northern China (Upper Yellow River): Implications for provenance and paleoenvironmental interpretations. CATENA 231, 107257, http://doi.org/10.1016/j.catena.2023.107257

Stinchcomb, G.E., Quade, J., Levin, N.E., Iverson, N., Dunbar, N., McIntosh, W., Arnold, L.J., Demuro, M., Duval, M., Grün, R., Zhao, J.-x., White, M., Hynek, S.A., Brown, F.H., Rogers, M.J., Semaw, S., 2023. Fluvial response to Quaternary hydroclimate in eastern Africa: Evidence from Gona, Afar, Ethiopia. Quaternary Science Reviews 309, 108083, http://doi.org/10.1016/j.quascirev.2023.108083

Svistunov, M.I., Kurbanov, R.N., Murray, A.S., Taratunina, N.A., Semikolennykh, D.V., Entin, A.L., Deev, Y.V., Zolnikov, I.D., Panin, A.V., 2022. Constraining the age of Quaternary megafloods in the Altai Mountains (Russia) using luminescence. Quaternary Geochronology 73, 101399, http://doi.org/10.1016/j.quageo.2022.101399

Utkina, A.O., Panin, A.V., Kurbanov, R.N., Murray, A.S., 2022. Unexpectedly old luminescence ages as an indicator of the origin of the upper Volga River valley sediments. Quaternary Geochronology 73, 101381, http://doi.org/10.1016/j.quageo.2022.101381

Wang, Y., Li, G., Wang, X., Yan, Z., Qin, C., Yang, J., Yang, H., Deng, Y., Pan, L., Chen, C., Zhao, W., Hou, G., 2022. Single-grain K-feldspar pIRIR dating of the Shalongka archeological site revealed the relationship between monsoon, overbank flooding, and human occupation during the Holocene on the northeastern Tibetan Plateau. Quaternary Science Reviews 298, 107848, http://doi.org/10.1016/j.quascirev.2022.107848

- glacial and periglacial

Kenzler, M., Gibb, M.A., Gehrmann, A., Deutschmann, A., Rother, H., Obst, K., Hüneke, H., 2023. Identification of Quaternary alluvial-fan deposits (Rügen, SW Baltic Sea): Significance for recognition of syn-kinematic sedimentation in glacitectonic complexes. Geomorphology 424, 108558, http://doi.org/10.1016/j.geomorph.2022.108558

Kumar, P., Sharma, M.C., Deswal, S., Manna, I., Chakraborty, E., Prakash, S., 2023. Last Glacial Maximum and subsequent glacial chronology in the monsoon-dominated Sikkim Himalaya, India. Palaeogeography, Palaeoclimatology, Palaeoecology 617, 111480, http://doi.org/10.1016/j.palaeo.2023.111480

Pánek, T., Březný, M., Smedley, R., Winocur, D., Schönfeldt, E., Agliardi, F., Fenn, K., 2023. The largest rock avalanches in Patagonia: Timing and relation to Patagonian Ice Sheet retreat. Quaternary Science Reviews 302, 107962, http://doi.org/10.1016/j.quascirev.2023.107962

Rex, C.L., Bateman, M.D., Buckland, P.C., Panagiotakopulu, E., Livingstone, S.J., Hardiman, M., Eddey, L., 2023. A revision of the British chronostratigraphy within the last glacial-interglacial cycle based on new evidence from Arclid, Cheshire UK. Quaternary Science Reviews 299, 107882, http://doi.org/10.1016/j.quascirev.2022.107882

Smith, L.N., Sohbati, R., Jain, M., 2023. Rock surface luminescence dating of gravel determines the age of a glacial outburst megaflood, Glacial Lake Missoula, Montana, USA. Geology 51, 323-328, http://doi.org/10.1130/G50721.1

- lacustrine

Hou, Y., Long, H., Tsukamoto, S., Gao, L., Zhang, J., Tamura, T., Frechen, M., 2023. Late Quaternary evolution of Daihai Lake in northern China and implications to the variation of the East Asian summer monsoon. Quaternary Science Reviews 309, 108097, http://doi.org/10.1016/j.quascirev.2023.108097

Wang, M., Wang, X., Pan, B., Yi, S., Van Balen, R., Zhao, Z., Dong, X., Vandenberghe, J., Wang, Y., Lu, H., 2023. Multiple paleolakes caused by glacier river-blocking on the southeastern Tibetan plateau in response to climate changes since the last glacial maximum. Quaternary Science Reviews 305, 108012, http://doi.org/10.1016/j.quascirev.2023.108012

- loess

Alberto Torres-Guerrero, C., Álvarez, D., Preusser, F., Ramón Olarieta, J., Poch, R.M., 2023. Evolution of soil porosity in loess-palaeosol sequences of the Ebro Valley, NE Iberia. CATENA 230, 107244, http://doi.org/10.1016/j.catena.2023.107244

Cheng, L., Yang, L., Long, H., Song, Y., Chen, Z., Lan, M., Xie, M., Dong, Z., 2023. Early Holocene dust activity variation in the southern Tibetan Plateau and its response to solar irradiance. Palaeogeography, Palaeoclimatology, Palaeoecology 620, 111561, http://doi.org/10.1016/j.palaeo.2023.111561

Cheng, L., Yang, L., Long, H., Zhang, J., Miao, X., Wu, Y., Lan, M., Song, Y., Dong, Z., 2023. Late Holocene change in South Asian monsoons and their influences on human activities in the southern Tibetan Plateau. CATENA 228, 107153, http://doi.org/10.1016/j.catena.2023.107153

Dave, A.K., Timar-Gabor, A., Kabacińska, Z., Scardia, G., Safaraliev, N., Nigmatova, S., Fitzsimmons, K.E., 2022. A Novel Proxy for Tracking the Provenance of Dust Based on Paired E1'-Peroxy Paramagnetic Defect Centers in Fine-Grained Quartz. Geophysical Research Letters 49, e2021GL095007, http://doi.org/10.1029/2021GL095007

Dave, A.K., Timar-Gabor, A., Scardia, G., Safaraliev, N., Fitzsimmons, K.E., 2022. Variation in Luminescence Characteristics and Paramagnetic Defect Centres in Fine-Grained Quartz From a Loess-Palaeosol Sequence in Tajikistan: Implications for Provenance Studies in Aeolian Environments. Frontiers in Earth Science 10, 835281, http://doi.org/10.3389/feart.2022.835281

Gu, Y., Lu, H., Hajdas, I., Haghipour, N., Zhang, H., Wu, J., Shao, K., 2023. Radiocarbon dating of small snail shells in a loess-palaeosol sequence at Mangshan, central China. CATENA 228, 107157, http://doi.org/10.1016/j.catena.2023.107157

Jiang, H.C., Yin, Q.Z., Berger, A., Wei, L.H., Wu, Z.P., Wei, X.T., Shi, W., 2023. Orbitally and galactic cosmic forced abrupt climate events during the last glacial period. Quaternary Science Reviews 301, 107921, http://doi.org/10.1016/j.quascirev.2022.107921

Kurbanov, R.N., Buylaert, J.P., Stevens, T., Taratunina, N.A., Belyaev, V.R., Makeev, A.O., Lebedeva, M.P., Rusakov, A.V., Solodovnikov, D., Költringer, C., Rogov, V.V., Streletskaya, I.D., Murray, A.S., Yanina, T.A., 2022. A detailed luminescence chronology of the Lower Volga loess-palaeosol sequence at Leninsk. Quaternary Geochronology 73, 101376, http://doi.org/10.1016/j.quageo.2022.101376

Li, Y., Song, Y., Fitzsimmons, K.E., Dave, A.K., Liu, Y., Zong, X., Sun, H., Liu, H., Orozbaev, R., 2022. Investigating Potential Links Between Fine-Grained Components in Loess and Westerly Airflow: Evidence From East and Central Asia. Frontiers in Earth Science 10, 901629, http://doi.org/10.3389/feart.2022.901629

Li, Y., Tsukamoto, S., Long, H., Zhang, J., Yang, L., 2022. Coarse-grained K-rich feldspar and fine-grained polymineral IRSL dating of loess-palaeosol from the Chinese Loess Plateau: A comparison. Quaternary Geochronology 73, 101379, http://doi.org/10.1016/j.quageo.2022.101379

Liu, X., Miao, X., Nie, J., Zhang, X., Wang, Y., Li, X., Ou, X., Lai, Z., 2023. Distribution and fate of Tibetan Plateau loess. CATENA 225, 107022, http://doi.org/10.1016/j.catena.2023.107022

Lomax, J., Wolf, D., Wolpert, U.T., Sahakyan, L., Hovakimyan, H., Faust, D., Fuchs, M., 2021. Establishing a Luminescence-Based Chronostratigraphy for the Last Glacial-Interglacial Cycle of the Loess-Palaeosol Sequence Achajur (Armenia). Frontiers in Earth Science 9, http://doi.org/10.3389/feart.2021.755084

Maleki, S., Khormali, F., Kehl, M., Azizi, G., Shahpouri, F., Shahbazi, R., Frechen, M., 2023. A loess-paleosol record of climate and vegetation change during the past 27,000 years from South-East of the Caspian Sea, Iran. Quaternary International 652, 1-16, http://doi.org/10.1016/j.quaint.2022.12.011

Meshcheryakova, O.A., Volvakh, N.E., Kurbanov, R.N., Zykina, V.S., Zykin, V.S., Murray, A.S., Volvakh, A.O., Malikov, D.G., Buylaert, J.P., 2022. The upper Pleistocene loess-palaeosol sequence at solonovka on the Cis-Altai plain, west Siberia – First luminescence dating results. Quaternary Geochronology 73, 101384, http://doi.org/10.1016/j.quageo.2022.101384

Volvakh, N.E., Kurbanov, R.N., Zykina, V.S., Murray, A.S., Stevens, T., Költringer, C.A., Volvakh, A.O., Malikov, D.G., Taratunina, N.A., Buylaert, J.P., 2022. First high-resolution luminescence dating of loess in Western Siberia. Quaternary Geochronology 73, 101377, http://doi.org/10.1016/j.quageo.2022.101377

Wang, L., Chen, S., Zhao, H., Li, S.-H., Zhang, J., 2023. Comparison of feldspar dating protocols for loess samples older than 70 ka from the Tianshan Mountains, arid central Asia. Quaternary International 652, 41-51, http://doi.org/10.1016/j.quaint.2023.01.014

Wu, C., Wang, Z., Wang, Q., Qian, P., Zheng, X., Wei, G., 2023. Sedimentary provenance and age of the Shengshan Island loess on the continental shelf of the East China Sea: Implications for windblown dust transport during the Last Glaciation. Geomorphology 427, 108624, http://doi.org/10.1016/j.geomorph.2023.108624

- marine

Liu, J., Qiu, J., Saito, Y., Zhang, X., Wang, H., Wang, F., Chen, L., Xu, G., Chen, B., Li, M., An, Y., 2023. Late Pleistocene to Holocene facies architecture and sedimentary evolution of the Zhejiang coast, East China Sea. Marine Geology 459, 107027, http://doi.org/10.1016/j.margeo.2023.107027

Yuan, X., Hu, R., Feng, X., Qiu, J., Wang, N., Yao, Z., Zhu, L., Li, J., 2023. Sedimentary records and implications for the evolution of sedimentary environments inferred from BH1302 during the late Quaternary in the Bohai Sea, China. Marine Geology 456, 106986, http://doi.org/10.1016/j.margeo.2022.106986

- soil

de Souza, J.J.L.L., de Castro, F.E., de Azevedo Andrade, C.V.P., Ker, J.C., Perez Filho, A., 2023. Brazilian semiarid soils formed during the last glacial maximum. CATENA 223, 106899, http://doi.org/10.1016/j.catena.2022.106899

Freire Guerra, M.D., Lelis Leal de Souza, J.J., Gonçalves Reynaud Schaefer, C.E., Nogueira de Souza, M.J., 2023. Remnant wetlands under palm swamps in the Araripe Plateau, Brazilian semiarid. CATENA 226, 107074, http://doi.org/10.1016/j.catena.2023.107074

- surface exposure dating

Freiesleben, T.H., Thomsen, K.J., Jain, M., 2023. Novel luminescence kinetic models for rock surface exposure dating. Radiation Measurements 160, 106877, http://doi.org/10.1016/j.radmeas.2022.106877

Freiesleben, T.H., Thomsen, K.J., Murray, A.S., Sohbati, R., Jain, M., Hvidt, S., Jakobsen, B., Aubry, T., 2022. Rock surface and sand-sized sediment quartz dating using optically stimulated luminescence of a Middle-to-Upper Palaeolithic sequence at the Bordes-Fitte rock shelter (Les Roches d'Abilly, Central France). Quaternary Geochronology 73, 101406, http://doi.org/10.1016/j.quageo.2022.101406

Semikolennykh, D.V., Cunningham, A.C., Kurbanov, R.N., Panin, A.V., Zolnikov, I.D., Deev, E.V., Murray, A.S., 2022. Dating of megaflood deposits in the Russian Altai using rock surface luminescence. Quaternary Geochronology 73, 101373, http://doi.org/10.1016/j.quageo.2022.101373

Smith, L.N., Sohbati, R., Jain, M., 2023. Rock surface luminescence dating of gravel determines the age of a glacial outburst megaflood, Glacial Lake Missoula, Montana, USA. Geology 51, 323-328, http://doi.org/10.1130/G50721.1

- tephra (and volcanic related)

Razum, I., Ilijanić, N., Petrelli, M., Pawlowsky-Glahn, V., Miko, S., Moska, P., Giaccio, B., 2023. Statistically coherent approach involving log-ratio transformation of geochemical data enabled tephra correlations of two late Pleistocene tephra from the eastern Adriatic shelf. Quaternary Geochronology 74, 101416, http://doi.org/10.1016/j.quageo.2022.101416

Zhang, S., Blockley, S., Armitage, S.J., Satow, C., Manning, C., Barzilai, O., Boaretto, E., White, D., Timms, R., 2023. Distal tephra reveal new MIS 5e Kos eruptions: Implications for the chronology and volcanic evolution histories in the Eastern Mediterranean region. Quaternary Science Reviews 307, 108054, http://doi.org/10.1016/j.quascirev.2023.108054

- thermochronology

Stalder, N.F., Biswas, R.H., Herman, F., 2022. Maximized erosion at the last glacial maximum revealed by thermoluminescence thermochronometry. Quaternary Geochronology 73, 101405, http://doi.org/10.1016/j.quageo.2022.101405

Archaeology applications

AeolianChen, X., He, A., Sun, X., Wei, Q., Liu, K., He, C., Liang, T., Yang, R., Wang, T., Shen, Z., Forestier, H., Zhou, Y., Li, Y., 2023. Guomo open-air site (15–12 ka) in Guangxi Zhuang Autonomous Region, southern China: A new cobble-based industry for rethinking the definition of "Hoabinhian". Journal of Archaeological Science: Reports 49, 104033, http://doi.org/10.1016/j.jasrep.2023.104033

Anil, D., Chauhan, N., Ajithprasad, P., Devi, M., Mahesh, V., Khan, Z., 2022. An Early Presence of Modern Human or Convergent Evolution? A 247 ka Middle Palaeolithic Assemblage from Andhra Pradesh, India. Journal of Archaeological Science: Reports 45, 103565, http://doi.org/10.1016/j.jasrep.2022.103565

Barbieri, A., Maier, A., Lauer, T., Mischka, C., Hattermann, M., Uthmeier, T., 2022. Post-LGM environments and foragers on the move: New data from the lower Altmühl Valley (Franconian Jura, SE Germany). Journal of Human Evolution 173, 103267, http://doi.org/10.1016/j.jhevol.2022.103267

Caruana, M.V., Wilson, C.G., Arnold, L.J., Blackwood, A.F., Demuro, M., Herries, A.I.R., 2023. A marine isotope stage 13 Acheulian sequence from the Amanzi Springs Area 2 Deep Sounding excavation, Eastern Cape, South Africa. Journal of Human Evolution 176, 103324, http://doi.org/10.1016/j.jhevol.2023.103324

del Val, M., Alonso, M.J., Duval, M., Arriolabengoa, M., Álvarez, I., Bodego, A., Cheng, H., Hermoso de Mendoza, A., Aranburu, A., Iriarte, E., 2022. Luminescence and ESR dating of the sedimentary infill from the multi-level cave system of Alkerdi-Zelaieta (Navarre, N Spain). Quaternary Geochronology 73, 101380, http://doi.org/10.1016/j.quageo.2022.101380

Doronicheva, E., Golovanova, L., Doronichev, V., Nedomolkin, A., Tregub, T., Volkov, M., Rusakov, A., Korzinova, A., Muriy, A., 2023. The MIS 4 environmental stress impact on hominin occupation in the northwestern Caucasus: New evidence from the Hadjoh 2 site. Journal of Archaeological Science: Reports 47, 103781, http://doi.org/10.1016/j.jasrep.2022.103781

Fazeli Nashli, H., Theodorakopoulou, K., Stamoulis, K., Athanassas, C., Nazari, H., Nokandeh, J., Jamshidi Yeganeh, S., Shokri, M., 2023. Deciphering the chronology of Tepe Sialk (South) "Ziggurat", North Central Iranian Plateau, through optically stimulated luminescence (OSL) dating. Journal of Archaeological Science: Reports 48, 103860, http://doi.org/10.1016/j.jasrep.2023.103860

Feathers, J.K., Frouin, M., Bench, T.G., 2022. Luminescence dating of Enigmatic rock structures in New England, USA. Quaternary Geochronology 73, 101402, http://doi.org/10.1016/j.quageo.2022.101402

Fonte, J., Rodrigues, A.L., Dias, M.I., Russo, D., Pereiro, T.d., Carvalho, J., Amorim, S., Jorge, C., Monteiro, P., Ferro-Vázquez, C., Costa-García, J.M., Gago, M., Oltean, I., 2023. Reassessing Roman military activity through an interdisciplinary approach: Myth and archaeology in Laboreiro Mountain (Northwestern Iberia). Journal of Archaeological Science: Reports 49, 103993, http://doi.org/10.1016/j.jasrep.2023.103993

Freiesleben, T.H., Thomsen, K.J., Murray, A.S., Sohbati, R., Jain, M., Hvidt, S., Jakobsen, B., Aubry, T., 2022. Rock surface and sand-sized sediment quartz dating using optically stimulated luminescence of a Middle-to-Upper Palaeolithic sequence at the Bordes-Fitte rock shelter (Les Roches d'Abilly, Central France). Quaternary Geochronology 73, 101406, http://doi.org/10.1016/j.quageo.2022.101406

García Sanjuán, L., Medialdea, A., Balsera Nieto, V., Athanassas, C., Pike, A., Standish, C.D., Dias, M.I., Rodrigues, A.L., Clavero Toledo, J.L., Wheatley, D.W., Cintas-Peña, M., 2023. A multimethod approach to the genesis of Menga, a World Heritage megalith. Quaternary Research 111, 1-20, http://doi.org/10.1017/qua.2022.33

Gliganic, L.A., Slack, M., Meyer, M.C., 2023. Tending to tradition: Dating stone arrangement maintenance in northwest Australia using optical methods. Journal of Archaeological Science: Reports 49, 104053, http://doi.org/10.1016/j.jasrep.2023.104053

L. Hilgen, S., Pop, E., Adhityatama, S., A. Veldkamp, T., W.K. Berghuis, H., Sutisna, I., Yurnaldi, D., Dupont-Nivet, G., Reimann, T., Nowaczyk, N., F. Kuiper, K., Krijgsman, W., B. Vonhof, H., Ekowati, D.R., Alink, G., Ni Luh Gde Dyah Mega, H., Drespriputra, O., Verpoorte, A., Bos, R., Simanjuntak, T., Prasetyo, B., Joordens, J.C.A., 2023. Revised age and stratigraphy of the classic Homo erectus-bearing succession at Trinil (Java, Indonesia). Quaternary Science Reviews 301, 107908, http://doi.org/10.1016/j.quascirev.2022.107908

Li, H., Li, Y., Yu, L., Tu, H., Zhang, Y., Sumner, A., Kuman, K., 2022. Continuous technological and behavioral development of late Pleistocene hominins in central South China: Multidisciplinary analysis at Sandinggai. Quaternary Science Reviews 298, 107850, http://doi.org/10.1016/j.quascirev.2022.107850

Liritzis, I., 2022. Optically stimulated luminescence dating using quartz: Remarks and a plea for fairness. Scientific Culture 8, 175-194, http://doi.org/10.5281/zenodo.5893296

Phuc, P.T., Hue, N.T.N., Hue, P.T., Anh, T.T., Kien, N.K.T., Son, L.T., Nguyen, L.L., Xuan, T.D., Dinh, V.-P., Long, N.H., Tiep, N.V., Vu, C.D., Thiem, L.N., Nguyen, N.-Q., Kiet, H.A.T., Hung, N.Q., Tuyen, L.A., 2023. Improved thermoluminescence dating for heterogeneous, multilayered, and overlapped architectures: A case study with the Oc Eo archaeological site in Vietnam. Journal of Archaeological Science 155, 105800, http://doi.org/10.1016/j.jas.2023.105800

Qiu, J., Jin, J., Wang, X., Wei, C., Zuo, X., Wei, J., 2022. OSL chronological evidence reveals one of the earliest island-type Neolithic sites in the coastal area of South China. The Holocene 33, 27-37, http://doi.org/10.1177/09596836221126126

Reed, K.S., Berger, U., Sharon, G., Porat, N., 2023. Radiometric dating of Southern Levant dolmens – Applying OSL to resolve an old debate. Journal of Archaeological Science: Reports 49, 104019, http://doi.org/10.1016/j.jasrep.2023.104019

Richard, M., 2023. Trapped Charge Dating and Archaeology, in: Pollard, A.M., Armitage, R.A., Makarewicz, C.A. (Eds.), Handbook of Archaeological Sciences. John Wiley & Sons Ltd., pp. 69-87, http://doi.org/10.1002/9781119592112.ch4

Silva-Sánchez, N., Tim, K., Fernández-Ferreiro, M., López-Salas, E., Turner, S., Sánchez-Pardo, J.-C., 2022. Written in soil and paper. Investigating environmental transformations of a monastic landscape by combining geoarchaeology and palynology with historical analysis at Samos (Spain). Journal of Archaeological Science: Reports 45, 103575, http://doi.org/10.1016/j.jasrep.2022.103575

Wang, Y., Zhang, X., Sun, X., Yi, S., Min, K., Liu, D., Yan, W., Cai, H., Wang, X., Curnoe, D., Lu, H., 2023. A new chronological framework for Chuandong Cave and its implications for the appearance of modern humans in southern China. Journal of Human Evolution 178, 103344, http://doi.org/10.1016/j.jhevol.2023.103344

White, J.T., Henry, A., Kuehn, S., Loso, M.G., Rasic, J.T., 2022. Terminal Pleistocene human occupation of the upper Copper River basin, southern Alaska: Results of test excavations at Nataeł Na'. Quaternary International 640, 23-43, http://doi.org/10.1016/j.quaint.2022.08.012

ESR, applied in various contexts

Dave, A.K., Timar-Gabor, A., Kabacińska, Z., Scardia, G., Safaraliev, N., Nigmatova, S., Fitzsimmons, K.E., 2022. A Novel Proxy for Tracking the Provenance of Dust Based on Paired E1'-Peroxy Paramagnetic Defect Centers in Fine-Grained Quartz. Geophysical Research Letters 49, e2021GL095007, http://doi.org/10.1029/2021GL095007

Dave, A.K., Timar-Gabor, A., Scardia, G., Safaraliev, N., Fitzsimmons, K.E., 2022. Variation in Luminescence Characteristics and Paramagnetic Defect Centres in Fine-Grained Quartz From a Loess-Palaeosol Sequence in Tajikistan: Implications for Provenance Studies in Aeolian Environments. Frontiers in Earth Science 10, 835281, http://doi.org/10.3389/feart.2022.835281

del Val, M., Alonso, M.J., Duval, M., Arriolabengoa, M., Álvarez, I., Bodego, A., Cheng, H., Hermoso de Mendoza, A., Aranburu, A., Iriarte, E., 2022. Luminescence and ESR dating of the sedimentary infill from the multi-level cave system of Alkerdi-Zelaieta (Navarre, N Spain). Quaternary Geochronology 73, 101380, http://doi.org/10.1016/j.quageo.2022.101380

Hernando-Alonso, I., Moreno, D., Ortega, A.I., Benito-Calvo, A., Alonso, M.J., Parés, J.M., Martínez-Fernández, A., Carbonell, E., Bermúdez de Castro, J.M., 2022. ESR chronology of the fluvial sequence of Cueva del Silo (Sierra de Atapuerca, Spain). Quaternary Geochronology 73, 101374, http://doi.org/10.1016/j.quageo.2022.101374

Ma, Z., Peng, T., Feng, Z., Li, X., Song, C., Wang, Q., Tian, W., Zhao, X., 2023. Tectonic and climate controls on river terrace formation on the northeastern Tibetan Plateau: Evidence from a terrace record of the Huangshui River. Quaternary International 656, 16-25, http://doi.org/10.1016/j.quaint.2022.11.004

Richard, M., 2023. Trapped Charge Dating and Archaeology, in: Pollard, A.M., Armitage, R.A., Makarewicz, C.A. (Eds.), Handbook of Archaeological Sciences. John Wiley & Sons Ltd., pp. 69-87, http://doi.org/10.1002/9781119592112.ch4

Basic research

Freiesleben, T.H., Thomsen, K.J., Jain, M., 2023. Novel luminescence kinetic models for rock surface exposure dating. Radiation Measurements 160, 106877, http://doi.org/10.1016/j.radmeas.2022.106877

Kitis, G., Pagonis, V., 2023. Simulation of thermoluminescence signals at very low dose rates and low doses: Implications for dosimetric applications. Radiation Physics and Chemistry 209, 110968, http://doi.org/10.1016/j.radphyschem.2023.110968

Kolb, T., Sontag-González, M., Fuchs, M., 2022. Testing the potential of a standardized growth curve approach for improving the applicability and performance of fading correction. Quaternary Geochronology 73, 101375, http://doi.org/10.1016/j.quageo.2022.101375

Lawless, J.L., Chen, R., Pagonis, V., 2023. A model explaining the anomalous fading effect in thermoluminescence (TL). Radiation Measurements 160, 106881, http://doi.org/10.1016/j.radmeas.2022.106881

Peng, J., Wang, X., Adamiec, G., Zhao, H., 2022. Critical role of the deep electron trap in explaining the inconsistency of sensitivity-corrected natural and regenerative growth curves of quartz OSL at high irradiation doses. Radiation Measurements 159, 106874, http://doi.org/10.1016/j.radmeas.2022.106874

Rahimzadeh, N., Zhang, J., Tsukamoto, S., Long, H., 2023. Characteristics of the quartz isothermal thermoluminescence (ITL) signal from the 375 °C peak and its potential for extending the age limit of quartz dating. Radiation Measurements 161, 106899, http://doi.org/10.1016/j.radmeas.2022.106899

Souza, P.E., Pupim, F.N., Mazoca, C.E.M., Río, I.d., Mineli, T.D., Rodrigues, F.C.G., Porat, N., Hartmann, G.A., Sawakuchi, A.O., 2023. Quartz OSL sensitivity from dating data for provenance analysis of pleistocene and holocene fluvial sediments from lowland Amazonia. Quaternary Geochronology 74, 101422, http://doi.org/10.1016/j.quageo.2023.101422

Williams, O.M., Spooner, N.A., 2023. Quartz defect pair model for exo-electron emission. Radiation Measurements 161, 106897, http://doi.org/10.1016/j.radmeas.2022.106897

Dosimetry

Karampiperi, M., Kazakis, N.A., 2023. Thermoluminescence characterization and kinetic parameters of eyeglass lenses for applications in retrospective/accidental dosimetry. Radiation Measurements 163, 106934, http://doi.org/10.1016/j.radmeas.2023.106934

Instruments

Goto, S., Hayashi, H., Yamaguchi, H., Sekiguchi, H., Akino, R., Shimizu, M., 2023. Signal-stabilized Al2O3:C-OSL dosimeter "checking chip" for correcting OSL reader sensitivity variation. Radiation Measurements 160, 106893, http://doi.org/10.1016/j.radmeas.2022.106893

Sontag-González, M., Mittelstraß, D., Kreutzer, S., Fuchs, M., 2022. Wavelength calibration and spectral sensitivity correction of luminescence measurements for dosimetry applications: Method comparison tested on the IR-RF of K-feldspar. Radiation Measurements 159, 106876, http://doi.org/10.1016/j.radmeas.2022.106876

Portable instruments

Rex, C.L., Bateman, M.D., Buckland, P.C., Panagiotakopulu, E., Livingstone, S.J., Hardiman, M., Eddey, L., 2023. A revision of the British chronostratigraphy within the last glacial-interglacial cycle based on new evidence from Arclid, Cheshire UK. Quaternary Science Reviews 299, 107882, http://doi.org/10.1016/j.quascirev.2022.107882

Robins, L., Roskin, J., Marder, O., Edeltin, L., Yu, L., Greenbaum, N., 2023. Geomorphic, environmental, and archeological significance of Last Glacial Maximum to middle Holocene dune damming, northwestern Negev dunefield margin, Israel. Quaternary Science Reviews 308, 108098, http://doi.org/10.1016/j.quascirev.2023.108098

Tipping, R., Bates, R., Cameron, A., Clarke, A., Duthie, S., Ewan, L., Kinnaird, T., Mann, B., Noble, G., Ross, I., Sabnis, H., Wickham-Jones, C., 2022. Environmental reconstruction and formation processes in a large Mesolithic lithic scatter at Nethermills of Crathes, Aberdeenshire, Scotland. Journal of Archaeological Science: Reports 45, 103605, http://doi.org/10.1016/j.jasrep.2022.103605

Review
Liritzis, I., 2022. Optically stimulated luminescence dating using quartz: Remarks and a plea for fairness. Scientific Culture 8, 175-194, http://doi.org/10.5281/zenodo.5893296

Mahan, S.A., Rittenour, T.M., Nelson, M.S., Ataee, N., Brown, N., DeWitt, R., Durcan, J., Evans, M., Feathers, J., Frouin, M., Guérin, G., Heydari, M., Huot, S., Jain, M., Keen-Zebert, A., Li, B., López, G.I., Neudorf, C., Porat, N., Rodrigues, K., Sawakuchi, A.O., Spencer, J.Q.G., Thomsen, K., 2023. Guide for interpreting and reporting luminescence dating results. GSA Bulletin 135, 1480-1502, http://doi.org/10.1130/B36404.1

Richard, M., 2023. Trapped Charge Dating and Archaeology, in: Pollard, A.M., Armitage, R.A., Makarewicz, C.A. (Eds.), Handbook of Archaeological Sciences. John Wiley & Sons Ltd., pp. 69-87, http://doi.org/10.1002/9781119592112.ch4

Ancient TL

Aims and Scope

Ancient TL is a journal devoted to Luminescence dating, Electron Spin Resonance (ESR) dating, and related techniques. It aims to publish papers dealing with experimental and theoretical results in this field, with a minimum of delay between submission and publication. Ancient TL also publishes a current bibliography, thesis abstracts, letters, and miscellaneous information, e.g., announcements for meetings.

Frequency

Two issues per annum in June and December

Submission of articles to Ancient TL

Ancient TL has a reviewing system in which direct dialogue is encouraged between reviewers and authors. For instructions to authors and information on how to submit to Ancient TL, please visit the website at:
http://ancienttl.org/TOC1.htm

Journal Enquiries

For enquiries please contact the editor:
Regina DeWitt, Department of Physics, East Carolina University, Howell Science Complex, 1000 E. 5th Street, Greenville, NC 27858, USA; Tel: +252-328-4980; Fax: +252-328-0753
(dewittr@ecu.edu)

Subscriptions to Ancient TL

Ancient TL Vol. 32 No.2 December 2014 was the last issue to be published in print. Past and current issues are available for download free of charge from the Ancient TL website:
http://ancienttl.org/TOC4.htm